HHS Public Access

Author manuscript

Heart Rhythm. Author manuscript; available in PMC 2016 October 01.

Published in final edited form as:

Heart Rhythm. 2015 October ; 12(10): 2115–2124. doi:10.1016/j.hrthm.2015.06.019.

Delayed afterdepolarizations generate both triggers and a vulnerable substrate promoting reentry in cardiac tissue

Michael B Liu, MS[1,2,#], **Enno de Lange, PhD**[1,5,#], **Alan Garfinkel, PhD**[1,2,3], **James N Weiss, MD**[1,2,3,4], and **Zhilin Qu, PhD**[1,2,*]

[1]The UCLA Cardiovascular Research Laboratory, David Geffen School of Medicine, University of California, Los Angeles, California 90095, USA [2]Department of Medicine (Cardiology), David Geffen School of Medicine, University of California, Los Angeles, California 90095, USA [3]Department of Integrative Biology and Physiology, David Geffen School of Medicine, University of California, Los Angeles, California 90095, USA [4]Department of Physiology, David Geffen School of Medicine, University of California, Los Angeles, California 90095, USA [5]Department of Knowledge Engineering, Maastricht University, 6200 MD Maastricht, The Netherlands

Abstract

Background—Delayed afterdepolarizations (DADs) have been well-characterized as arrhythmia triggers but their role in generating a tissue substrate vulnerable to reentry is not well understood.

Objective—To test the hypothesis that random DADs can self-organize to generate both an arrhythmia trigger and a vulnerable substrate simultaneously in cardiac tissue as a result of gap junction coupling.

Methods—Computer simulations in one-dimensional cable and two-dimensional tissue models were carried out. The cellular DAD amplitude was varied by changing the strength of sarcoplasmic reticulum Ca release. Random DAD latency and amplitude in different cells were simulated using Gaussian distributions.

Results—Depending on the strength of spontaneous sarcoplasmic reticulum Ca release and other conditions, random DADs in cardiac tissue resulted in the following behaviors: 1) triggered activity (TA); 2) a vulnerable tissue substrate causing unidirectional conduction block and reentry by inactivating Na channels; 3) both triggers and a vulnerable substrate simultaneously by generating TA in regions next to regions with subthreshold DADs susceptible to unidirectional conduction block and reentry. The probability of the latter two behaviors was enhanced by

*Correspondence to: Zhilin Qu, PhD, Department of Medicine, Division of Cardiology, David Geffen School of Medicine at UCLA, A2-237 CHS, 650 Charles E. Young Drive South, Los Angeles, CA 90095, Tel: 310-794-6050, Fax: 310-206-9133, zqu@mednet.ucla.edu.

#These authors contributed equally

Conflicts of interest: None

reduced Na channel availability, reduced gap junction coupling, increased tissue heterogeneity, and less synchronous DAD latency.

Conclusions—DADs can self-organize in tissue to generate arrhythmia triggers, a vulnerable tissue substrate, and both simultaneously. Reduced Na channel availability and gap junction coupling potentiate this mechanism of arrhythmias, which are relevant to a variety of heart disease conditions.

Keywords

delayed afterdepolarization; conduction block; reentry; arrhythmias; computer simulation

Introduction

Delayed afterdepolarizations (DADs) are transient depolarizations in the diastolic phase following an action potential (AP) that have been linked to arrhythmogenesis in cardiac diseases [1-3]. Experimental studies have revealed that the primary cause of DADs is spontaneous sarcoplasmic reticulum (SR) calcium (Ca) release, which activates Ca-sensitive inward currents such as the Na-Ca exchange current to depolarize diastolic membrane potential. Ca waves are promoted under Ca overload conditions in normal myocytes [4, 5] or under diseased conditions, such as heart failure [6-8], ischemia [9], catecholaminergic polymorphic ventricular tachycardia (CPVT) [10], and long QT syndromes [11, 12].

The role of DADs in arrhythmogenesis is generally explained as follows: when the amplitude of a DAD is above a certain threshold (termed a *suprathreshold* DAD), it can trigger an AP, called triggered activity (TA), which can cause a premature ventricular contraction (PVC) to trigger reentrant or focal arrhythmias [3, 13]. However, not all DADs are large enough to trigger APs, and the role of these *subthreshold* DADs in arrhythmogenesis is not well understood. It is well known that elevation of resting membrane potential can cause conduction slowing and block [14]. Elevation of the resting membrane potential of a ventricular myocyte will first enhance conduction by moving the potential closer to the sodium (Na) channel activation threshold, but further elevation will slow conduction due to Na channel inactivation. In an experimental study, Rosen et al [15] showed that impulses occurring during a DAD in a Purkinje fiber did not propagate to the ventricles, whereas earlier or later impulses did, suggesting that DADs can cause conduction block in Purkinje fibers. However, to our knowledge, no other studies have been carried out to investigate the role of subthreshold DADs as causes of conduction block and/or reentry.

The amplitude and latency of diastolic Ca waves tend to vary irregularly from beat-to-beat due to random properties of spontaneous SR Ca release [5, 16, 17], which can be further enhanced because of cell-to-cell or regional heterogeneities in Ca cycling properties [3, 18]. However, myocytes in cardiac tissue are coupled via gap junctions which tends to smooth the voltage differences between adjacent cells, synchronizing their depolarizations locally. These two competing factors could interact to generate regions of tissue with suprathreshold DADs causing TA bordering on regions with subthreshold DADs susceptible to conduction block, initiating reentry.

Based on this reasoning, we hypothesized that depending on the SR Ca release strength and other conditions, random DADs can self-organize in tissue to cause: 1) arrhythmia triggers by generating PVCs; 2) a vulnerable tissue substrate causing unidirectional conduction block of a PVC; and 3) both simultaneously resulting in initiation of reentry. To test this hypothesis, we performed computer simulations in one-dimensional (1D) cables and two-dimensional (2D) tissue models. DADs were simulated by commanded SR Ca releases, similar to DADs induced in experiments by caffeine pulses [19] or local β-adrenergic agonist application [20]. Random DAD latency was simulated by randomly setting the SR Ca release time, and the amplitude of DAD was changed by varying the strength of the SR Ca release flux. The effects of Na channel availability, gap junction coupling, as well as other factors, were characterized.

Methods

Simulations were carried out in 1D cable and 2D tissue models. The partial differential equation governing voltage is

$$\frac{\partial V}{\partial t} = -I_{ion}/C_m + D\left(\frac{\partial^2 V}{\partial x^2}+\frac{\partial^2 V}{\partial y^2}\right) \quad (1)$$

where V is the membrane voltage, C_m=1 μF/cm^2 is the membrane capacitance, and D is the diffusion constant (proportional to gap junction conductance) with its control value set as 0.0005 cm^2/ms. The AP model and generation of DADs were described previously by Xie et al [21]. The spontaneous SR Ca release strength is described by a parameter g_{spon} and the random latency of the release follows a Gaussian distribution of standard deviation σ. More details of the model and simulation methods were present in *Supplemental Materials*.

In the simulations, unless specified the maximum Na channel conductance (g_{Na}) was 12 pA/pF and the Na channel steady-state inactivation curve (h_∞) was left-shifted 5 mV, i.e., the $V_{1/2}$ was changed from −66 mV to −71 mV. Fig.1A shows example traces of DADs and TA for different g_{spon} values and Fig.1B shows the maximum voltage versus g_{spon}. The threshold for suprathreshold DADs or TA in a single cell was g_{spon}=0.066 ms^{-1} (arrow in Fig.1B) without the shift of h_∞ but with a 5 mV left-shift, it increased to 0.0695 ms^{-1}.

Results

Effects of subthreshold DADs

Subthreshold DADs can cause conduction block when Na channel availability is reduced—We simulated a 1D cable in which the middle one-third of the cells exhibited DADs (Fig.2). We assumed that the spontaneous Ca releases causing DADs were identical and occurred at the same time in each cell (Fig.2A). A premature stimulus was applied to the first 10 cells at the end of the cable, and the ability of the AP to propagate to the other end of the cable was studied for different DAD amplitudes (adjusted by varying g_{spon}) and coupling intervals. For normal Na channel properties in our model, subthreshold DADs failed to cause conduction block, regardless of DAD amplitude or coupling interval. However, if Na channel availability was reduced by shifting the half-maximal voltage of steady-state

inactivation (described by h_∞) in the negative direction, as might occur physiologically with PKA, PKC or CaMKII phosphorylation of Na channels [22] or in some Brugada syndrome mutations [23], conduction block occurred over a range of coupling intervals when DAD amplitude reached a critical range (Fig. 2B and C). In this range, the DAD-induced depolarization caused sufficient Na channel inactivation to result in conduction failure. Fig. 2D illustrates the time course of Na channel availability (h*j) during a DAD with a peak voltage around −70 mV for control (solid) and for a 5 mV left-shift of h_∞ (dashed), showing that a 5 mV left-shift causes a large reduction in Na channel availability during the DAD. As the DAD amplitude was increased further (g_{spon}>0.0695 ms^{-1}), TA occurred in the DAD region, which propagated in both directions and collided retrogradely with the premature beat. Fig.2E plots the region of conduction block versus the left-shift of h_∞ and g_{Na}, showing that reducing g_{Na} also promoted conduction block.

Effects of random DAD latency—In the simulations in Fig.2, the spontaneous Ca releases causing a DAD in the mid-region of the cable all occurred synchronously by design. To study the effects of random DAD latency, we simulated a 1D cable in which the latency of the spontaneous Ca release event for each cell was randomly assigned from a Gaussian distribution. Gap junction coupling naturally smoothed the resulting DAD in the tissue (Fig. 3A). Unlike the non-random case in Fig.2, a premature beat with a fixed coupling interval could either block or propagate successfully through the DAD region depending on the particular randomization pattern of the trial (Fig.3B). In Figs.3C-E, we show the probability of conduction failure through the DAD region versus the strength of spontaneous Ca release (g_{spon}) for different standard deviations (σ) of the Gaussian distribution of latencies, g_{Na}, and gap junction coupling. Increasing σ caused conduction block to occur over a broader range of g_{spon}. Note that in the non-random case, TA occurred when g_{spon}>0.0695 ms^{-1} and no conduction block occurred. With random latency, a higher g_{spon} was required to trigger APs due to the source-sink effects, and conduction block still occurred when g_{spon} >0.0695 ms^{-1}. Reducing g_{Na} increased the probability of conduction block, while reducing gap junction coupling had a small effect.

If we applied the same deterministic or random DAD distribution as in the 1D cables (Figs. 2 and 3) to 2D tissue, reentry could be induced by a premature stimulus (see Online Movie 1 and Movie 2).

Combined effects of supra- and sub-threshold DADs

In the simulations shown above, external paced premature stimuli were used to illustrate how DADs can cause conduction block. We next examined whether TA self-generated by DADs could develop conduction block in the same cable due to random latency of DADs in different regions causing both subthreshold and suprathreshold DADs.

Complex excitation patterns in 1D cable—We carried out simulations in a homogeneous 1D cable with random DAD latency as in Fig.3 without externally paced premature stimuli. Complex excitation patterns occurred, which could be classified into three categories: 1) subthreshold DADs without TA (Fig.4A); 2) suprathreshold DADs causing TA which propagated successfully along the cable without conduction block (Fig.

4B); and 3) suprathreshold DADs causing TA which propagated partway before developing conduction block (Fig.4C). Fig.4D shows the probability of the three behaviors as a function of DAD amplitude (g_{spon}). No TA occurred when g_{spon} was small, but as g_{spon} increased the incidence of TA also increased (dashed in Fig.4D). Due to random latency and cell coupling, the g_{spon} threshold for TA was higher in tissue than in a single cell (g_{spon}>0.0695 ms^{-1}). Figs.4E-H show that the probability of block increases with broadened latency distribution (Fig.4E), decreased cell coupling (Fig.4F), reduced g_{Na} (Fig.4G), and left-shifted h_{∞} (Fig. 4H).

Reentry initiation in 2D tissue—Unidirectional conduction block of DAD-mediated TA in the 1D cable raises the possibility that under similar conditions in 2D tissue, reentry may be induced when conduction block is appropriately localized. Analogous to the 1D simulations in Figs.3 and 4, we first simulated a homogeneous 2D tissue in which all cells were identical with the same DAD amplitude (i.e., identical g_{spon}) but DAD latencies were randomly assigned following a Gaussian distribution. Both subthreshold DADs and TA were observed, but in over 10,000 simulations using different parameter settings, reentry was never observed, even when g_{Na} or gap junction coupling was reduced.

Since Ca release properties in real cardiac tissue are not homogeneous, we then performed simulations in which g_{spon} was varied in random checkerboard patterns, drawing from a Gaussian distribution, as illustrated in Fig.5A. Checker sizes ranged from 1×1 to 256×256 cells. The DAD latencies were still varied randomly from cell to cell as in the simulations above. We observed three behaviors (Fig.5B): all DADs are subthreshold (no TA); DADs induce TA without reentry formation (TA without reentry), and DADs induce TA with reentry formation (TA with reentry). Fig.5C shows the probability of these different behaviors versus the checker size for control parameters. For large checker sizes, the majority of the simulations exhibited TA without reentry (i.e., PVCs only), and a small number of the simulations exhibited reentry. As the checker size decreased, the probability of TA without reentry decreased, while that of subthreshold DADs increased. Interestingly, the probability of reentry first increased and then decreased to zero at small checker sizes. Reducing gap junction conductance selectively increased the probability of reentry at large and small checker sizes (Fig.5D), but suppressed reentry at intermediate checker sizes. Reducing Na channel conductance g_{Na} in steps from 16 to 8 pS/pF increased the probability of reentry particularly at large checker sizes, while further reduction to 6 pS/pF suppressed reentry due to low excitability (Fig.5E). Fig.5F compares the probability of TA with and without reentry versus g_{Na}. As g_{Na} was reduced, the probability of TA without reentry decreased while the probability of TA with reentry first increased then decreased. We also performed simulations in which g_{spon} was varied randomly in checkerboard patterns, but DAD latency was fixed. We never observed reentry, indicating that the random DAD latency is a key property promoting reentry. This was also supported by simulations investigating the effect of DAD latency distribution on reentry in 2D tissue, which depended sensitively on σ (online Fig.S1).

Finally, we examined how electrical remodeling in heart failure affects DAD-mediated arrhythmogenesis (Fig.6). Electrical remodeling decreased the threshold of g_{spon} required for conduction block (Fig.6A) and greatly decreased the g_{spon} required for TA with reentry

(Fig.6B). Similar to Fig.5F, decreasing g_{Na} reduced the probability of TA without reentry and first increased then decreased the probability of TA with reentry (Fig.6C).

As shown in Figs.5 and 6, checker size had a non-monotonic effect on probability of reentry. A possible explanation is illustrated in Fig. 7, which shows voltage snapshots for three different checker sizes with reduced gap junction coupling. For the 256×256 case (Fig.7A and Online Movie 3), the randomness of DAD latency resulted in nonuniform DAD voltages in a single checker, allowing conduction in one direction but block in another direction at the borders of the individual checkers. Due to the large checker size, there was enough room for the broken wavefronts to turn and reenter the checker from another direction. For the 32×32 case (Fig.7B and Online Movie 4), TA that formed in the individual checkers tended to propagate neatly in all directions and fuse together, such that there was not enough unexcited tissue for a broken wavefront to form a spiral wave. For the 1×1 case (Fig.7C and Online Movie 5), the checkers with high g_{spon} values were not large enough to generate TA individually unless neighboring checkers also had randomly been assigned large enough g_{spon} values to overcome the source-sink mismatch. This effectively resulted in large heterogeneous regions with or without TA, increasing the probability of reentry. Note that when the gap junction coupling was normal, however, no reentry could occur for the 1×1 case (Fig.5C).

Discussion

DADs are classically recognized as triggers of PVCs that can initiate reentry when they encounter a vulnerable tissue substrate. Here we demonstrate that subthreshold DADs can also directly generate a tissue substrate vulnerable to unidirectional conduction block. Moreover, DAD-induced triggers and substrates can occur simultaneously in the same tissue to induce reentry. These effects are enhanced with reduced Na channel availability and gap junction coupling, with electrical remodeling changes in heart failure, and when regional differences in Ca cycling properties underlying DADs are accentuated, as occurs in the setting of heart diseases. Our observations thus provide novel insights into DAD-related arrhythmogenesis.

Roles of DADs in cardiac arrhythmogenesis

Based on observations in the present study, we can summarize the roles of DADs in cardiac arrhythmogenesis as follows:

DADs generate arrhythmia triggers—The well-known effect of suprathreshold DADs in cardiac arrhythmogenesis is their ability to trigger an AP and generate TA, which can cause focal (non-reentrant) arrhythmias or serve as PVCs to initiate reentrant arrhythmias [1-3, 24, 25].

DADs generate a vulnerable substrate—Traditionally, dispersion of excitability and/or refractoriness make a tissue vulnerable to initiation of reentry by a trigger such as a PVC [26]. Unidirectional conduction block initiating reentry occurs either because the Na current has not recovered sufficiently from inactivation to overcome the source-sink mismatch of neighboring repolarized cells (dispersion of excitability) or the neighboring

cells are still in a refractory state (dispersion of refractoriness). In this study, we have demonstrated that subthreshold DADs can cause unidirectional conduction block via the former mechanism by elevating diastolic membrane potential and inactivating Na channels sufficiently to cause conduction block. The random distribution of DAD latency increases the probability of conduction block (Fig.3) because as DAD latency distribution becomes wider, DAD duration in the tissue prolongs, giving more time for more Na channels to inactivate.

Since subthreshold DADs can occur at any time during diastole, a very late diastolic subthreshold DAD could potentially cause regional conduction block of a subsequent sinus beat, initiating reentry directly from sinus rhythm in the absence of a PVC. In this case, the first beat of reentrant ventricular tachycardia would have the same QRS morphology as subsequent tachycardia beats, which is frequently observed in clinical studies [27]. Thus, unlike reentrant arrhythmias induced by dispersion of refractoriness in which an external PVC is usually required, DAD-mediated reentrant arrhythmias do not necessarily require an external PVC, as the next sinus beat can serve to initiate reentry.

DADs simultaneously generate triggers and a vulnerable substrate—Due to random [5, 16, 17] and heterogeneous [3, 18] Ca release, DADs in tissue can lead to complex depolarization patterns in which some regions generate suprathreshold DADs causing TA, while other regions generate subthreshold DADs promoting regional conduction block and initiation of reentry (Figs.4-7). TA generated in one region may propagate in all or only in one direction, or be blocked a distance away such that reentry can result if the broken wavefronts have enough available excitable tissue. Although the interactions among random latency, heterogeneity, gap junction coupling and Na channel availability are complex, the probability of conduction block and reentry increases for reduced gap junction coupling, Na current availability and electrical remodeling. Our simulations also show that both random latency and heterogeneous Ca release are needed for reentry to occur.

Clinical relevance

As shown in our simulations (Figs. 4-6), a negative shift in the steady state inactivation curve and/or reduction of the maximal Na conductance increased the probability of conduction block and reentry in the presence of DADs. This condition is physiologically mimicked by PKA-and/or PKC-mediated phosphorylation of Na channels during sympathetic stimulation or CaMKII-mediated phosphorylation of Na channels in the setting of heart failure [22], Na channel remodeling in ischemic heart disease [28] or loss-of-function Na channel mutations in Brugada syndrome [23] and other diseases [29].

Since Class I antiarrhythmic agents not only reduce the Na channel open probability but also left-shift the steady-state inactivation curve [30], this may have been a contributing factor to the proarrhythmic effects of Na channel blockers observed in the CAST trial [31]. In the CAST trial, Na channel blockers effectively suppressed PVCs by more than 80%, but mortality nevertheless increased due to more frequent lethal arrhythmic events. Many later studies established that blocking the Na channel is proarrhythmic in ischemic and infarcted tissue, due to lowered excitability and increased post-repolarization refractoriness in the

border zone [28, 30]. Our simulations suggest that an additional mechanism could also be important: if the PVCs in these patients originated from Ca wave-mediated DADs, then reducing excitability by blocking Na channels could have reduced the frequency of benign PVCs by converting suprathreshold DADs to subthreshold DADs, while at the same time paradoxically increasing the probability that the less frequent remaining suprathreshold DADs will initiate reentry. This phenomenon was illustrated in Figs. 5 F and 6 C, in which reducing Na channel conductance reduced the incidence of TA without reentry (benign PVCs) but increased the probability of TA with reentry (malignant PVCs initiating VT/VF) over a certain range of g_{Na}.

Finally, PVCs can originate from either the His-Purkinje system or ventricular myocardium in patients, and may exhibit simple patterns in the ECG, such as fixed QRS morpohology (unifocal PVCs) and fixed coupling interval, or complex patterns such as different QRS morphologies (multifocal PVCs) and varying coupling intervals (modulated parasystole). For the mechanisms described in this study, we can speculate that PVCs arising from an abnormal area in the His-Purkinje system would tend to produce unifocal PVCs with some degree of variation in coupling intervals. In ventricular tissue, on the other hand, the random process by which Ca waves in individual myocytes self-organize to generate suprathreshold vs. subthreshold DADs in different regions of tissue would likely produce multifocal PVCs with variable coupling intervals. Another potential insight from the current study relates to the hypothesis subthreshold DADs occurring in ventricles may be one of the mechanisms underlying U-waves in the ECG [32], as supported by recent experimental studies [13]. Based on our finding that subthreshold DADs also can create vulnerable substrate for reentry, it is intriguing to speculate that PVCs accompanying U-waves in the ECG may confer a higher arrhythmia risk than when U-waves are absent.

Limitations

A limitation of this study is that the DADs in our model were caused by commanded SR Ca releases with randomly distributed amplitude and/or latency following Gaussian distributions, which allowed us to readily control DAD amplitude and latency. To realistically simulate spontaneous Ca release via the mechanism of Ca-induced Ca release and the feedback between Ca and voltage requires a detailed Ca cycling model incorporating random RyR openings [5, 33, 34]. However, since we studied only the effects of voltage depolarization on conduction block and not the feedback between Ca and voltage or other excitation-contraction dynamics, the simulation results from the present study still provides important mechanistic insights into arrhythmias caused by DADs. We altered DAD amplitude by increasing spontaneous SR Ca release, but DAD amplitude can also be regulated by the diastolic Ca-voltage coupling gain [35], which we did not study except in the context of heart failure electrical remodeling (Fig. 6). We also did not explicitly study the effects of altering DAD duration at the cellular level, which in real cells is sensitive to the subcellular location and numbers of sites from which Ca waves originate. Our 1D and 2D tissue models are relatively simple compared to real tissue, and the results may influenced by specific structural features of the tissue. For example, as shown in Fig.5, the proarrhythmic effects of blocking Na channels or reducing gap junction conductance depended on the specific spatial characteristics of heterogeneities. Nevertheless, the insights

from computer modeling in this study have uncovered novel mechanisms for DAD-mediated arrhythmogenesis that provide testable hypotheses for future experimental studies.

Conclusions

Whereas suprathreshold DADs in cardiac tissue generate triggers for reentrant arrhythmias, subthreshold DADs can create regions susceptible to unidirectional conduction block, directly increasing the probability that the triggers will induce reentry. This scenario is unlikely when Na channel properties are normal, but becomes increasingly probable as Na channel availability is reduced by sympathetic stimulation, disease-related remodeling, loss-of-function genetic defects, or Class I antiarrhythmic drugs, and as gap junction coupling is reduced by gap junction remodeling or fibrosis. These dynamics provide novel mechanistic insights into DAD-mediated arrhythmogenesis potentially relevant to a spectrum of cardiac diseases such as chronic ischemia, heart failure, Brugada syndrome and CPVT, as well as the proarrhythmic effects of Na channel blockers.

Supplementary Material

Refer to Web version on PubMed Central for supplementary material.

Acknowledgements

Supported by NIH/National Heart, Lung and Blood Institute grants P01 HL078931, R01 HL110791, the UCLA MSTP grant T32 GM008042 (to M.B.L.), the Swiss Foundation for Grants in Biology and Medicine grant PASMP3-127312 (to E.d.L.), and the Laubisch and Kawata endowments.

Abbreviations

DAD	delayed afterdepolarization
PVC	premature ventricular contraction
AP	action potential
CPVT	catecholaminergic polymorphic ventricular tachycardia
TA	triggered activity
SR	sarcoplasmic reticulum
1D	one-dimensional
2D	two-dimensional
Ca	calcium
Na	sodium

References

1. Rosen MR, Moak JP, Damiano B. The clinical relevance of afterdepolarizations. Ann N Y Acad Sci. 1984; 427:84–93. [PubMed: 6378020]
2. January CT, Fozzard HA. Delayed afterdepolarizations in heart muscle: mechanisms and relevance. Pharmacol Rev. 1988; 40:219–227. [PubMed: 3065793]

3. Katra RP, Laurita KR. Cellular mechanism of calcium-mediated triggered activity in the heart. Circ Res. 2005; 96:535–542. [PubMed: 15718502]
4. Cheng H, Lederer MR, Lederer WJ, Cannell MB. Calcium sparks and [Ca2+]i waves in cardiac myocytes. Am J Physiol. 1996; 270:C148–159. [PubMed: 8772440]
5. Nivala M, Ko CY, Nivala M, Weiss JN, Qu Z. Criticality in intracellular calcium signaling in cardiac myocytes. Biophys J. 2012; 102:2433–2442. [PubMed: 22713558]
6. Yeh YH, Wakili R, Qi XY, et al. Calcium-handling abnormalities underlying atrial arrhythmogenesis and contractile dysfunction in dogs with congestive heart failure. Circ Arrhythm Electrophysiol. 2008; 1:93–102. [PubMed: 19808399]
7. Pogwizd SM, Bers DM. Calcium cycling in heart failure: the arrhythmia connection. J Cardiovasc Electrophysiol. 2002; 13:88–91. [PubMed: 11843491]
8. Hoeker GS, Katra RP, Wilson LD, Plummer BN, Laurita KR. Spontaneous calcium release in tissue from the failing canine heart. Am J Physiol Heart Circ Physiol. 2009; 297:H1235–1242. [PubMed: 19648256]
9. Ross JL, Howlett SE. ß-adrenoceptor stimulation exacerbates detrimental effects of ischemia and reperfusion in isolated guinea pig ventricular myocytes. Eur J Pharmacol. 2009; 602:364–372. [PubMed: 19056376]
10. Watanabe H, Chopra N, Laver D, et al. Flecainide prevents catecholaminergic polymorphic ventricular tachycardia in mice and humans. Nat Med. 2009; 15:380–383. [PubMed: 19330009]
11. Mohler PJ, Schott J-J, Gramolini AO, et al. Ankyrin-B mutation causes type 4 long-QT cardiac arrhythmia and sudden cardiac death. Nature. 2003; 421:634–639. [PubMed: 12571597]
12. Burashnikov A, Antzelevitch C. Acceleration-induced action potential prolongation and early afterdepolarizations. J Cardiovasc Electrophysiol. 1998; 9:934–948. [PubMed: 9786074]
13. Morita H, Zipes DP, Morita ST, Wu J. Mechanism of U wave and polymorphic ventricular tachycardia in a canine tissue model of Andersen-Tawil syndrome. Cardiovasc Res. 2007; 75:510–518. [PubMed: 17531215]
14. Singer DH, Lazzara R, Hoffman BF. Interrelationship between automaticity and conduction in Purkinje fibers. Circ Res. 1967; 21:537–558. [PubMed: 6057710]
15. Rosen MR, Wit AL, Hoffman BF. Electrophysiology and pharmacology of cardiac arrhythmias. IV. Cardiac antiarrhythmic and toxic effects of digitalis. Am Heart J. 1975; 89:391–399. [PubMed: 1090138]
16. Wasserstrom JA, Shiferaw Y, Chen W, et al. Variability in timing of spontaneous calcium release in the intact rat heart is determined by the time course of sarcoplasmic reticulum calcium load. Circ Res. 2010; 107:1117–1126. [PubMed: 20829511]
17. Fujiwara K, Tanaka H, Mani H, Nakagami T, Takamatsu T. Burst Emergence of Intracellular Ca2+ Waves Evokes Arrhythmogenic Oscillatory Depolarization via the Na+−Ca2+ Exchanger: Simultaneous Confocal Recording of Membrane Potential and Intracellular Ca2+ in the Heart. Circ Res. 2008; 103:509–518. [PubMed: 18635824]
18. Plummer BN, Cutler MJ, Wan X, Laurita KR. Spontaneous calcium oscillations during diastole in the whole heart: the influence of ryanodine reception function and gap junction coupling. Am J Physiol Heart Circ Physiol. 2011; 300:H1822–H1828. [PubMed: 21378143]
19. Schlotthauer K, Bers DM. Sarcoplasmic reticulum Ca(2+) release causes myocyte depolarization. Underlying mechanism and threshold for triggered action potentials. Circ Res. 2000; 87:774–780. [PubMed: 11055981]
20. Myles RC, Wang L, Kang C, Bers DM, Ripplinger CM. Local β-Adrenergic Stimulation Overcomes Source-Sink Mismatch to Generate Focal Arrhythmia. Circ Res. 2012; 110:1454–1464. [PubMed: 22539768]
21. Xie Y, Sato D, Garfinkel A, Qu Z, Weiss JN. So little source, so much sink: requirements for afterdepolarizations to propagate in tissue. Biophys J. 2010; 99:1408–1415. [PubMed: 20816052]
22. Herren AW, Bers DM, Grandi E. Post-translational modifications of the cardiac Na channel: contribution of CaMKII-dependent phosphorylation to acquired arrhythmias. Am J Physiol Heart Circ Physiol. 2013; 305:H431–445. [PubMed: 23771687]

23. Hu D, Barajas-Martinez H, Burashnikov E, et al. A Mutation in the β3 Subunit of the Cardiac Sodium Channel Associated With Brugada ECG Phenotype. Circulation: Cardiovascular Genetics. 2009; 2:270–278. [PubMed: 20031595]
24. Pogwizd SM, Bers DM. Cellular basis of triggered arrhythmias in heart failure. Trends Cardiovasc Med. 2004; 14:61–66. [PubMed: 15030791]
25. Rubart M, Zipes DP. Mechanisms of sudden cardiac death. J Clin Invest. 2005; 115:2305–2315. [PubMed: 16138184]
26. Qu Z, Weiss JN. Mechanisms of Ventricular Arrhythmias: From Molecular Fluctuations to Electrical Turbulence. Annu Rev Physiol. 2015; 77:29–55. [PubMed: 25340965]
27. Saeed M, Link MS, Mahapatra S, et al. Analysis of intracardiac electrograms showing monomorphic ventricular tachycardia in patients with implantable cardioverter-defibrillators. Am J Cardiol. 2000; 85:580–587. [PubMed: 11078271]
28. Pu J, Boyden PA. Alterations of Na+ currents in myocytes from epicardial border zone of the infarct heart: A possible ionic mechanism for reduced excitability and postrepolarization refractoriness. Circ Res. 1997; 81:110–119. [PubMed: 9201034]
29. Grant AO, Carboni MP, Neplioueva V, et al. Long QT syndrome, Brugada syndrome, and conduction system disease are linked to a single sodium channel mutation. The Journal of Clinical Investigation. 2002; 110:1201–1209. [PubMed: 12393856]
30. Pu JL, Balser JR, Boyden PA. Lidocaine action on Na+ currents in ventricular myocytes from the epicardial border zone of the infarcted heart. Circ Res. 1998; 83:431–440. [PubMed: 9721700]
31. Echt DS, Liebson PR, Mitchell LB, et al. Mortality and morbidity in patients receiving encainide, flecainide, or placebo. The Cardiac Arrhythmia Suppression Trial. N Engl J Med. 1991; 324:781–788. [PubMed: 1900101]
32. Surawicz B. U wave: facts, hypotheses, misconceptions, and misnomers. J Cardiovasc Electrophysiol. 1998; 9:1117–1128. [PubMed: 9817564]
33. Chen W, Asfaw M, Shiferaw Y. The Statistics of Calcium-Mediated Focal Excitations on a One-Dimensional Cable. Biophys J. 2012; 102:461–471. [PubMed: 22325268]
34. Song Z, Ko Christopher Y, Nivala M, Weiss James N, Qu Z. Calcium-Voltage Coupling in the Genesis of Early and Delayed Afterdepolarizations in Cardiac Myocytes. Biophys J. 2015; 108:1908–1921. [PubMed: 25902431]
35. Maruyama M, Joung B, Tang L, et al. Diastolic intracellular calcium-membrane voltage coupling gain and postshock arrhythmias: role of purkinje fibers and triggered activity. Circ Res. 2010; 106:399–408. [PubMed: 19926871]

Clinical Perspectives

DADs are well known as arrhythmia triggers, but their role in creating a vulnerable tissue substrate for reentry has not been comprehensively investigated. In this study, we show that DADs that do not reach threshold for triggered activity can create a vulnerable tissue substrate by regionally decreasing excitability sufficiently to cause conduction block. Moreover, when both subthreshold and suprathreshold DADs coexist in the same tissue, the combination of triggers and a vulnerable substrate can lead directly to reentry initiation. These effects are enhanced when Na channel availability and gap junction coupling are reduced and tissue heterogeneities are enhanced, as occurs in the setting of heart disease. Since reduced Na channel availability potentiates this mechanism, Na channel blocking drugs may also be proarrhythmic by this mechanism.

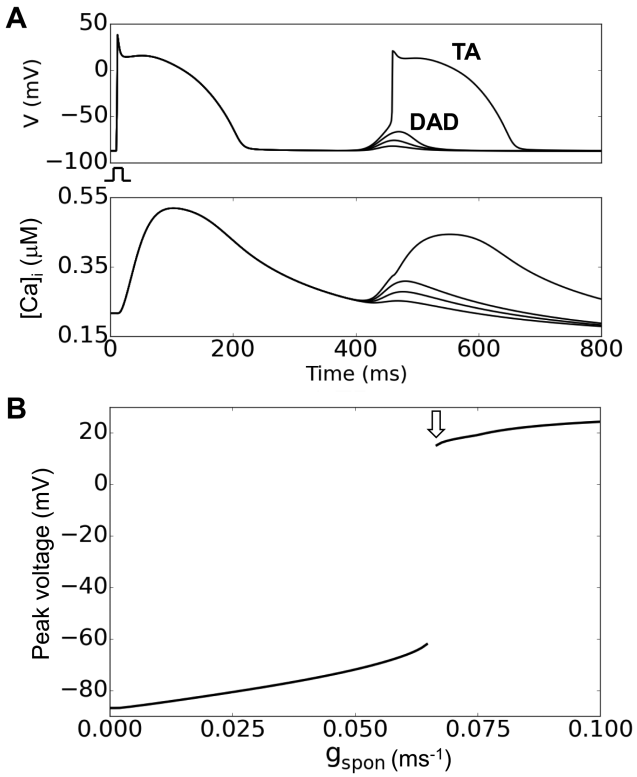

Figure 1. The DAD model

A. DADs and TA from a single isolated cell for different g_{spon} values. Upper traces show membrane potential and lower traces show the corresponding intracellular Ca concentrations. **B**. Maximum DAD voltage amplitude versus g_{spon}. The arrow indicates the g_{spon} threshold for a suprathreshold DAD eliciting TA.

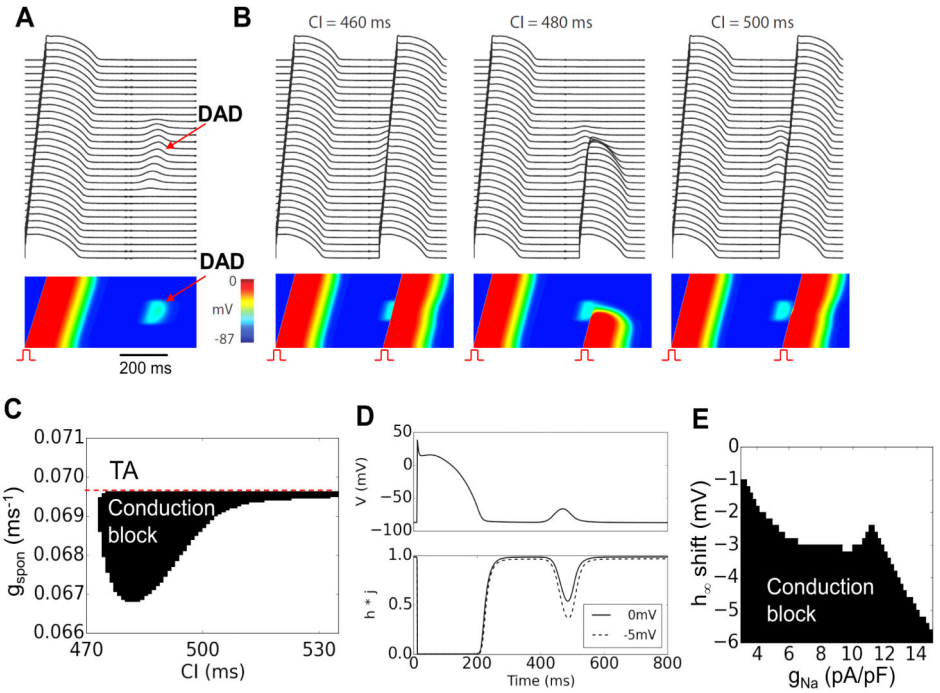

Figure 2. Conduction block due to a subthreshold DAD in a 1D cable

A. A 300 cell cable is paced at a cycle length of 500 ms and a subthreshold DAD occurs in the middle 100 cells approximately 450 ms after the AP upstroke. Upper traces show membrane potential of every 10th cell, and lower trace shows a space-time plot of voltage along the cable. **B**. Under the same conditions, a premature stimulus elicited an AP (PVC) which propagated into the DAD region. When the coupling interval (CI) of the PVC was 460 ms (left panel) or 500 ms (right panel), the PVC propagated successfully to the other end of the cable. For the CI of 480 ms (middle panel), however, conduction block occurred in the DAD region. **C**. A parameter diagram showing conduction block (in black) as a function of CI and g_{spon}. Dashed line indicates the transition from a subthreshold to suprathreshold DAD causing TA at g_{spon}=0.0695 ms^{-1}. **D**. Voltage and Na channel availability (h*j) versus time for the un-shifted (solid) and 5 mV left-shifted (dashed) h_∞ during a DAD. **E**. Conduction block as a function of g_{Na} and left-shift of h_∞.

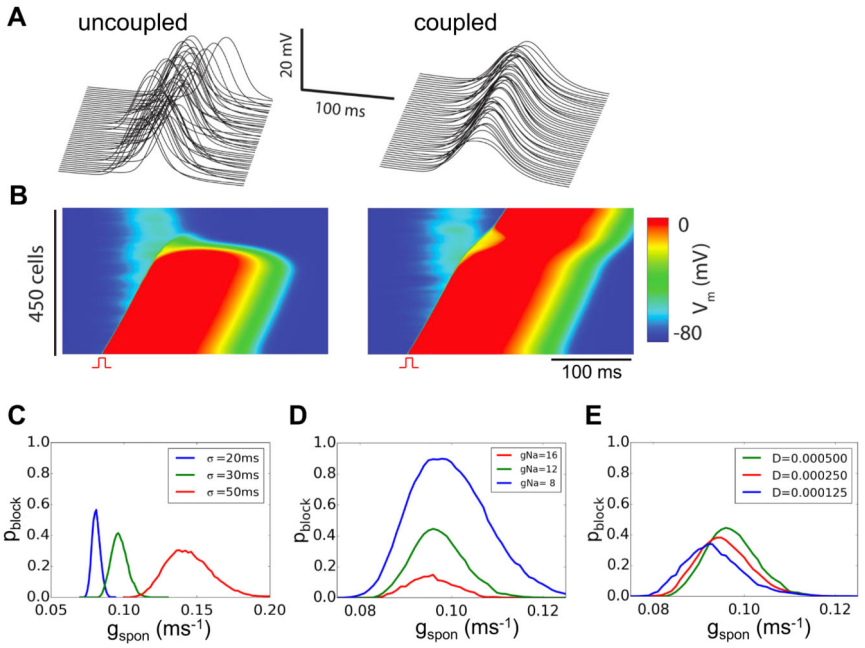

Figure 3. Effects of DAD synchronization on conduction block

A. Random DAD latency when the cells in a 1D cable are electrically uncoupled (left) or coupled by gap junctions (right), illustrating the synchronizing effect of coupling on the tissue DAD. **B**. Voltage snapshots showing two different trials in which DAD latencies were randomly selected from a Gaussian distribution with a standard deviation (σ) of 20 ms. The resulting subthreshold tissue DADs were sufficiently different to cause an identically-timed PVC to block in one trial (left), but successfully propagate in the other trial (right). **C-E**. Probability of conduction block (p_{block}) versus g_{spon} for different σ (C), g_{Na} (D), and D (E) in a cable length of 450 cells. The probability of each parameter point was calculated from 1,000 random trials. The green curve in C-E is the control case with σ=30 ms, D=0.0005 cm^2/ms, g_{Na}=12 pA/pF, and a −5 mV shift of h_∞.

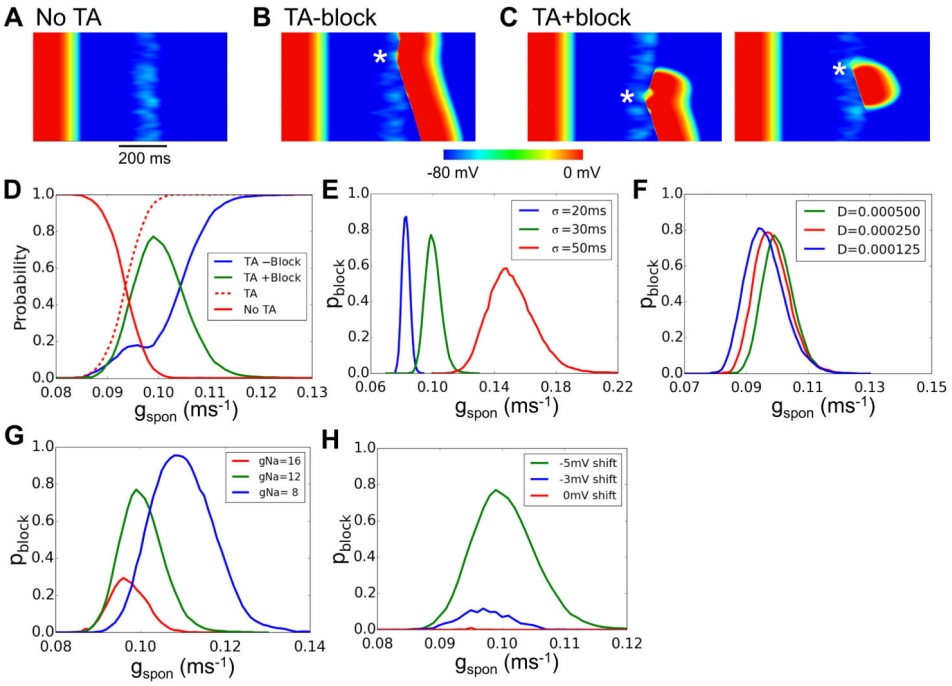

Figure 4. Complex excitation patterns in a 1D cable

A-C. Space-time plots of membrane potential versus time in a 300 cell cable in which all cells exhibited DADs with randomly assigned latencies (σ=50 ms) following a paced AP. g_{spon}=0.15 ms^{-1}. **D**. Probability of no TA (red), a successfully propagating TA (blue) and a TA with conduction block (green) versus g_{spon} for σ=30 ms. Arrow indicates the g_{spon} threshold for TA. **E**. Probability of conduction block versus g_{spon} for different σ. **F**. Probability of conduction block versus g_{spon} for different diffusion coefficients (D) reflecting gap junction coupling. **G**. Probability of conduction block versus g_{spon} for different g_{Na}. **H**. Probability of conduction block versus g_{spon} for shifts in the half-maximal voltage of h_{∞}. The cable length in D-H was 450 cells. The probability of each parameter point was calculated from 1,000 random trials. The green curve in D-H is the control case with σ=30 ms, D=0.0005 cm^2/ms, g_{Na}=12 pA/pF, and a −5 mV shift of h_{∞}.

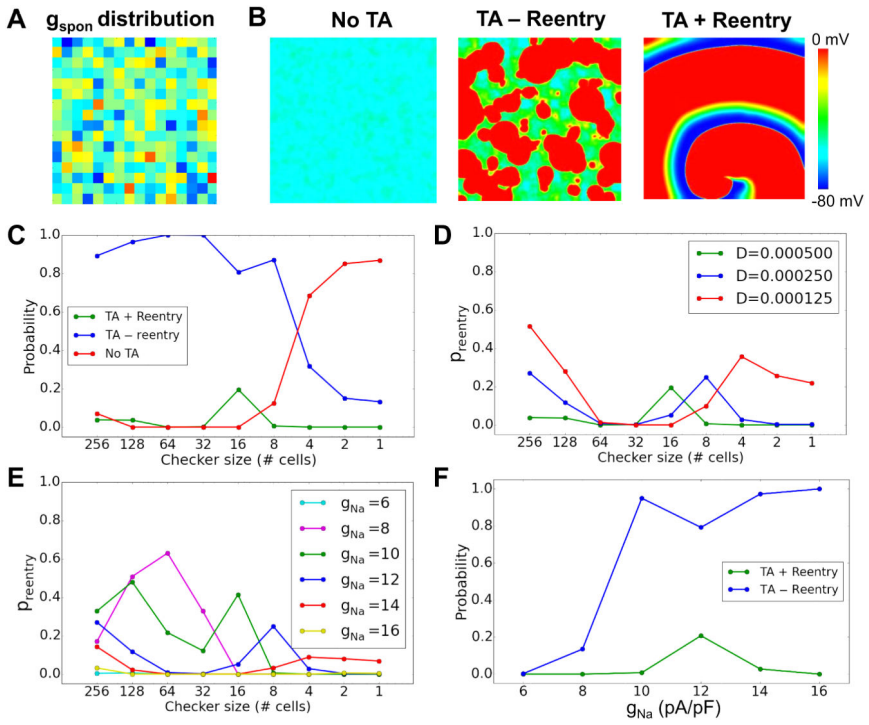

Figure 5. Summary data for reentry induction in heterogeneous 2D tissue

A. An example of checkerboard g_{spon} distribution. g_{spon} in each checker was drawn from a random Gaussian distribution with an average value of 0.172 ms^{-1} and a standard deviation σ=0.03 ms^{-1}. **B**. Examples of voltage snapshots illustrating no TA, TA-reentry, and TA +reentry. **C**. Probability of TA+reentry (green), TA-reentry (blue), and no TA (red) versus checker size. The dashed line is the total probability of TA. **D**. Probability of reentry versus checker size for different diffusion coefficients (D, cm^2/ms). **E**. Probability of reentry for different g_{Na}. **F**. Probability of TA-reentry and TA+reentry versus g_{Na} for an 8×8 checker size. The standard deviation for random DAD latency of individual cells was σ=50 ms. The tissue size was 512 × 512 cells. The probability of each parameter point was calculated from 500 random trials.

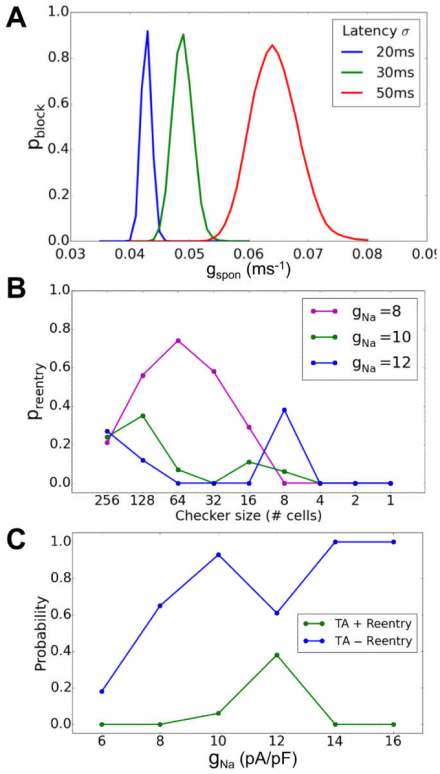

Figure 6. Conduction block and reentry in heart failure

Heart failure was simulated as described in Xie et al [21]. **A.** Probability of conduction block in a 1D cable versus g_{spon} for different DAD latency σ. The g_{spon} range for conduction block is lower than in the non-failing condition (Fig.4E). **B.** Probability of TA+reentry (green) versus checker size in a 2D tissue of failing cells for different g_{Na}. g_{spon} was drawn from a Gaussian distribution with an average value of 0.065 ms^{-1} and a standard deviation of σ=0.02 ms^{-1}. The DAD latency standard deviation σ=50 ms. **C**. Probability of TA-reentry and TA+reentry versus g_{Na}.

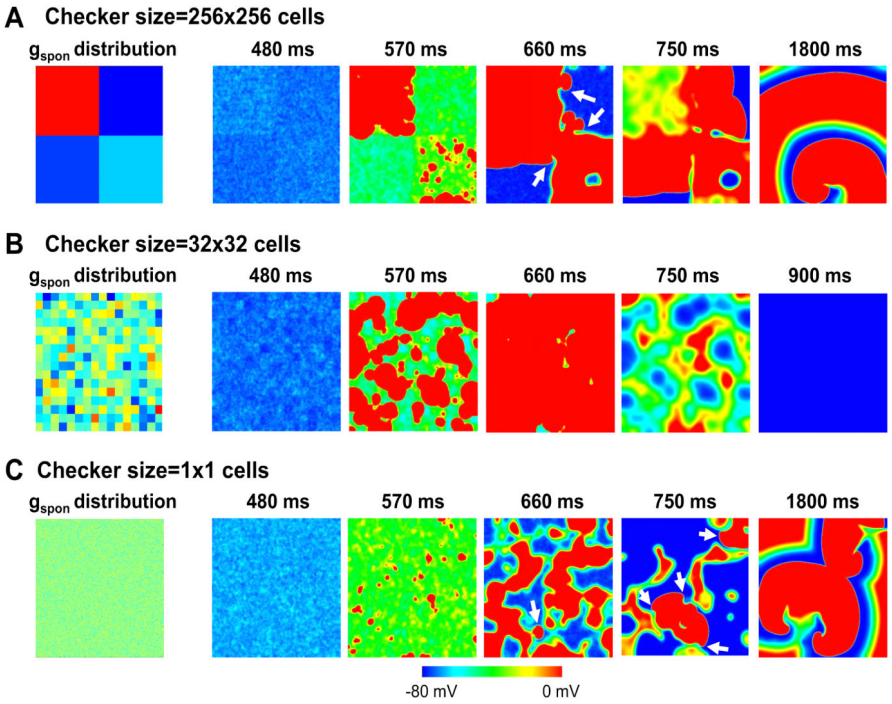

Figure 7. Voltage snapshots for three different checker sizes in heterogeneous 2D tissue

Left panels show the g_{spon} distributions and right panels show corresponding voltage snapshots of DAD-mediated TA and conduction block at various times following a paced AP, with checker sizes of 256×256 (**A**), 32×32 (**B**), and 1×1 cells (**C**).